tically short bond lengths (*17*).
15. K. Luth and S. Scheiner, *Int. J. Quantum Chem. Symp.* **26**, 817 (1992); A. T. Pudzianowski, *J. Chem. Phys.* **102**, 8029 (1995).
16. A. R. Grimm, G. B. Bacskay, A. D. Haymet, *Mol. Phys.* **86**, 369 (1995); S. S. Xantheas, *J. Am. Chem. Soc.* **117**, 10373 (1995). In both papers, table 1 provides an extensive compilation of structural parameters obtained from standard quantum chemical calculations.
17. K. Laasonen, F. Csajka, M. Parrinello, *Chem. Phys. Lett.* **194**, 172 (1992); F. Sim, A. St.-Amant, I. Papai, D. R. Salahub, *J. Am. Chem. Soc.* **114**, 4391 (1992); R. N. Barnett and U. Landman, *Phys. Rev. B* **48**, 2081 (1993), see sect. IIIB (ii).
18. D. Marx and M. Parrinello, *Z. Phys. B* **95**, 143 (1994); *J. Chem. Phys.* **104**, 4077 (1996); M. E. Tuckerman, D. Marx, M. L. Klein, M. Parrinello, *ibid.*, p. 5579. We used the staging transformation of the nuclear variables and sufficient thermostatting, following M. E. Tuckerman, G. J. Martyna, M. L. Klein, B. J. Berne, *J. Chem. Phys.* **99**, 2796 (1993).
19. D. Marx and M. Parrinello, *Nature* **375**, 216 (1995); *Science* **271**, 179 (1996).
20. R. P. Feynman, *Statistical Mechanics: A Set of Lectures* (Benjamin/Cummings, Reading, MA, 1972); D. Chandler and P. G. Wolynes, *J. Chem. Phys.* **74**, 4078 (1981).
21. R. Car and M. Parrinello, *Phys. Rev. Lett.* **55**, 2471 (1985).
22. The electronic structure was calculated within density functional theory with the use of the generalized gradient approximation BLYP [A. D. Becke, *Phys. Rev. A* **38**, 3098 (1988); C. Lee, W. Yang, R. G. Parr, *Phys. Rev. B* **37**, 785 (1988)], which yields excellent results for liquid water [M. Sprik, J. Hutter, M. Parrinello, *J. Chem. Phys.* **105**, 1142 (1996)], in particular for the O···O separation. The core electrons were eliminated with the use of pseudopotentials [N. Troullier and J. L. Martins, *Phys. Rev. B* **43**, 1993 (1991)], and the valence orbitals were expanded in plane waves up to 70 rydberg. The resulting optimized $H_5O_2^+$ (*23*) and $H_3O_2^-$ (*24*) geometries are in good agreement with those from correlated quantum chemical calculations (*12, 16*). The path integral was represented by 16 discrete replicas, and the complexes, placed in an isolated cubic box measuring 15 atomic units on a side, were coupled to a Nosé-Hoover bath at 300 K. Runs of 12,000 and 30,000 steps were carried out for the path integral simulations of $H_5O_2^+$ and $H_3O_2^-$, respectively. The corresponding classical runs contained roughly twice as many time steps as the quantum runs. In all cases, a time step of 0.17 fs was used.
23. The following data characterize $H_5O_2^+$: $r_{OH}^{min} = 0.98$ Å, $\langle r_{OH}\rangle_c = 0.98 \pm 0.03$ Å, $\langle r_{OH}\rangle_q = 0.99 \pm 0.07$ Å; $r_{OH^*}^{min} = 1.22$ Å, $\langle r_{OH^*}\rangle_c = 1.23 \pm 0.09$ Å, $\langle r_{OH^*}\rangle_q = 1.25 \pm 0.14$ Å; $R_{OO}^{min} = 2.43$ Å, $\langle R_{OO}\rangle_c = 2.44 \pm 0.06$ Å, $\langle R_{OO}\rangle_q = 2.45 \pm 0.09$ Å; $\angle_{OH^*O}^{min} = 173°$. Here r denotes distance, and $\angle$ denotes an angle. The superscript "min" specifies the structure at the minimum of the potential energy surface, and $\langle\ \rangle_c$ and $\langle\ \rangle_q$ denote statistical averages (first moments of distributions) at 300 K in the classical and quantum canonical ensembles, respectively, with the root-mean-square widths (from second moments) of the distributions following the ± signs. A comparison using radial distribution functions also reinforces our finding that the classical and quantum $H_5O_2^+$ complexes show strikingly similar characteristics at 300 K, with the quantum fluctuations resulting in slightly broader distributions, as expected.
24. The following data characterize $H_3O_2^-$: $r_{OH}^{min} = 0.97$ Å, $\langle r_{OH}\rangle_c = 0.97 \pm 0.03$ Å, $\langle r_{OH}\rangle_q = 0.99 \pm 0.07$ Å; $r_{O_aH^*}^{min} = 1.13$ Å, $r_{O_bH^*}^{min} = 1.39$ Å, $\langle r_{O_aH^*}\rangle_c = 1.07 \pm 0.05$ Å, $\langle r_{O_bH^*}\rangle_c = 1.53 \pm 0.13$ Å, $\langle r_{O_aH^*}\rangle_q = \langle r_{O_bH^*}\rangle_q = 1.28 \pm 0.05$ Å; $R_{OO}^{min} = 2.52$ Å, $\langle R_{OO}\rangle_c = 2.59 \pm 0.10$ Å, $\langle R_{OO}\rangle_q = 2.54 \pm 0.09$ Å; $\angle_{O_aH^*O_b}^{min} = 178°$. For notation see (*23*).
25. B. Halle and G. Karlström, *J. Chem. Soc. Faraday Trans. 2* **79**, 1031 (1983).
26. M.E.T. and M.L.K. would like to acknowledge support from NSF grants ASC95-04076 and CHE96-20317, and D.M. is grateful to T. Haymet for stimulating discussions. All calculations were performed either on site at the Center for Molecular Modeling or at the Cornell and Maui supercomputing centers on the IBM SP2 parallel machines.

23 October 1996; accepted 17 December 1996

Direct Measurement of a Tethered Ligand-Receptor Interaction Potential

Joyce Y. Wong,* Tonya L. Kuhl, Jacob N. Israelachvili, Nasreen Mullah, Samuel Zalipsky

Many biological recognition interactions involve ligands and receptors that are tethered rather than rigidly bound on a cell surface. A surface forces apparatus was used to directly measure the force-distance interaction between a polymer-tethered ligand and its receptor. At separations near the fully extended tether length, the ligands rapidly lock onto their binding sites, pulling the ligand and receptor together. The measured interaction potential and its dynamics can be modeled with standard theories of polymer and colloidal interactions.

In many biological systems, ligands are attached to the ends of flexible or semiflexible tether groups rather than fixed or immobilized on a surface or macromolecule. In many systems designed for selective targeting, flexible tethers are used. For example, in sterically stabilized liposomes (*1*), a fraction of the lipid head groups of a liposome are modified with a poly(ethylene glycol) (PEG) chain that has a targeting moiety attached at the extremity. The presence of the PEG chain increases the in vivo circulation time (*2*) essentially by steric stabilization (*3*), whereas the targeting moiety provides specificity. It is not known, however, how the presence of a flexible tether—which normally would be in a coiled state—alters the ligand-receptor interaction potential.

We have directly measured the interaction potential between a tethered ligand and its receptor. We chose the well-characterized receptor-ligand system of streptavidin-biotin. After immobilizing streptavidin on a supported lipid bilayer (*4*), we measured the interaction force-distance (*F-D*) profile with an opposing supported bilayer surface containing biotin tethered to the distal end of lipid-PEG (henceforth, PEG-biotin) (*5*) (Fig. 1) using the surface forces apparatus technique (*6*).

The effect of the PEG tether on the streptavidin-biotin interaction force profile is shown in Fig. 2, with a schematic representation in Fig. 3. As expected, we observed a weakly repulsive electrostatic "double-layer" force at large separations arising from the net negative charge on both the PEG-biotin and streptavidin surfaces (Fig. 3A and inset to Fig. 2). The magnitude and range of the repulsive electrostatic interaction can be fitted by standard theory based on the Poisson-Boltzmann equation and values for the potential of biotin (−55 mV) and streptavidin (−51 mV) (*4*). The interaction of the tethered biotin-streptavidin system is quite different from that of the untethered system. When the ligand and receptor are both rigidly bound to their respective surfaces, the ligand-receptor interaction is intrinsically of very short range (<5 Å) (Fig. 2, solid curve). Conversely, with the ligand attached to the end of a free polymer-like chain, there is a large attractive force (*7*) whose range corresponds directly with the fully extended length of the PEG chain with its biotin group, $L \approx 160$ Å (Fig. 2, point B, and Fig. 3B). This observation leads us to conclude that the end of the polymer chain freely samples all distances up to full extension, but, when the terminal ligand comes within 5 Å of its streptavidin binding site, the specific, short-range interaction locks in. The resulting tension in the almost fully extended polymer chain then pulls the surfaces together (Fig. 3, B → C).

With respect to the dynamic aspects of this kind of binding interaction, theories of end-grafted polymer chains have predicted that the free chain ends are, on average, located at a distance of $0.7R_F$ from the anchoring surface, where $R_F = 35$ Å is the Flory radius for a PEG-2000 tether (Fig. 1). However, the chain can experience a fluctuation that will allow it to explore all possible configurations, including near-full extension. For a particle diffusing in an external potential, $E_{ext}(D)$, the typical exploration time, τ, is given by

$$\tau(D) = \tau_0 \exp[E_{ext}(D)/kT] \qquad (1)$$

where k is the Boltzmann constant and T is temperature (their product being the thermal energy). If the intrinsic relaxation rate of

J. Y. Wong, T. L. Kuhl, J. N. Israelachvili, Department of Chemical Engineering, University of California, Santa Barbara, CA 93106, USA.
N. Mullah and S. Zalipsky, Sequus Pharmaceuticals, 960 Hamilton Court, Menlo Park, CA 94025, USA.

*To whom correspondence should be addressed. E-mail: jywong@engineering.ucsb.edu

a single chain, τ_0, is given by the Zimm time

$$\tau_0 \approx \frac{\eta R_F^3}{kT} \approx 10^{-8}\ \mathrm{s} \qquad (2)$$

where η is the viscosity of water and $E_{ext}(D)$ for $D > R_F$ is the parabolic potential

$$E_{ext}(D) = \frac{(D/R_F)^2 kT}{2} \qquad (3)$$

(8), the typical exploration time for a PEG-2000 chain to sample a configuration near full extension is $\tau = 10^{-8} \exp(12.5) = 10^{-3}$ s, that is, τ is in the millisecond range. This time is much shorter than our measuring time resolution and is consistent with the observation of a rapid locking-on. However, it is still much shorter than the time it would take two complementary binding sites, each rigidly attached to a bulky enzyme complex or membrane surface, to find each other.

On the first approach, the surfaces jump in from $D \approx 150$ Å $\approx L$ to a distance of $D \approx 43$ Å $\approx R_F$ (Fig. 2, point C). This distance corresponds roughly to the equilibrium thickness of a compressed polymer layer of chains that have one end bound to a surface (9). At this point in the interaction, there is a mixed population of polymer chains: The chains located on the outer edge of the contact zone are stretched, whereas those closer to the center are under compression (compare with Fig. 1B). With decreasing separation below R_F, the competition of, respectively, attractive and increasingly repulsive forces from the polymer chains determines the locations of the minimum and repulsive walls in the interaction profile.

Strong ligand-receptor bonds are essentially irreversible (the streptavidin-biotin bond energy is $\sim 35kT$), and, as two bonded surfaces are separated, breakage occurs not at the ligand-receptor bond but at the weakest part of the system—which in many cases is the supporting membrane, anchoring molecule, or tethering lipid (10). In the present system, separation at the membrane involves pullout of the anchoring biotin-PEG-lipids from the bilayer (Fig. 3D) because the force required to pull out a biotin-PEG-lipid, F_{lip}, is lower than the force needed to break a streptavidin-biotin bond (11). That lipid pullout occurred on separation was established by the flat shape of the potential well (see below) and also by the observation that on subsequent approaches the interaction was not the same (that is, irreversible): The surfaces still jumped in from the same separation of ~150 Å, but the final contact positions grew farther out with each new approach (43 Å on the first, 55 Å on the second, 60 Å on the third, and so on).

The highly unusual U-shape of the measured interaction potential, characterized by three distinct regions (C → D, D → E, and E → B in Fig. 3), can be readily shown to be

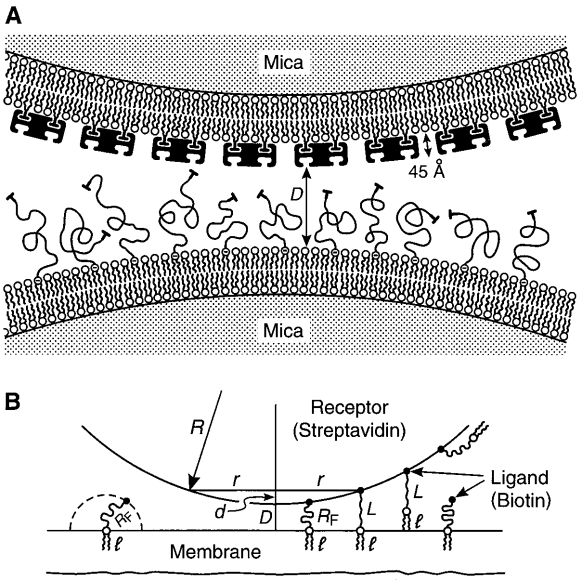

Fig. 1. (**A**) Schematic illustration of the PEG-biotin and streptavidin molecular configurations. The PEG-biotin coverage is 950 Å^2 per molecule or 4.5 mol% and corresponds to the so-called "weakly overlapping mushroom regime"; D corresponds to the distance from the outer edge of the streptavidin layer to the outer lipid head group surface on the opposing surface. The lipid head groups of PEG-biotin are negatively charged and the biotin molecule itself is neutral; the streptavidin protein is negatively charged at pH 7.2. (**B**) Schematic illustration of the relevant parameters used in the calculation of the interaction force profile (Fig. 3). The tether length L for the fully extended PEG-2000 chain is 153 Å, and the PEG-biotin molecules used in this study have a polydispersity [from matrix-assisted laser desorption/ionization (MALDI)] of 1.0018.

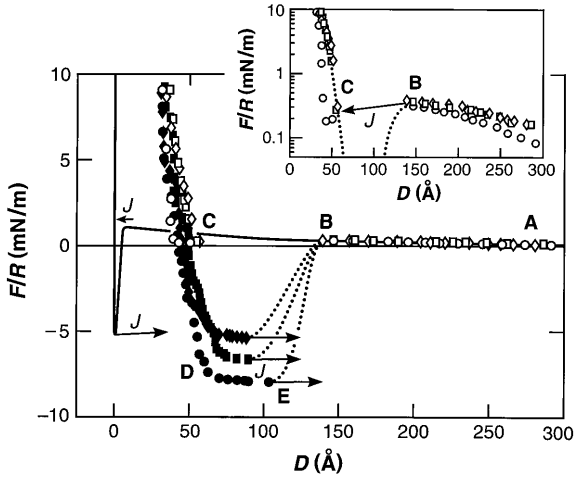

Fig. 2. Interaction force profile as a function of separation distance for streptavidin and PEG-biotin normalized by the radius of curvature, R. The force profile was measured at pH 7.2, 0.5 mM Na^+, and 25°C [below the solid-liquid transition temperature of dilauroylphosphatidylethanolamine (DLPE) (melting temperature T_m = 30°C) and DSPE (74°C) (16)]. The solid curve shows the interaction between streptavidin with 5% biotin without the PEG tether (17). Symbols: first approach (○) and separation (●); second approach (□) and separation (■); third approach (◇) and separation (◆). Arrows J denote inward and outward jumps on approach and separation, respectively. The inset shows the weakly repulsive, electrostatic "double-layer" force. The data are highly reproducible in comparisons of different contact positions within the same experiment as well as between different experiments.

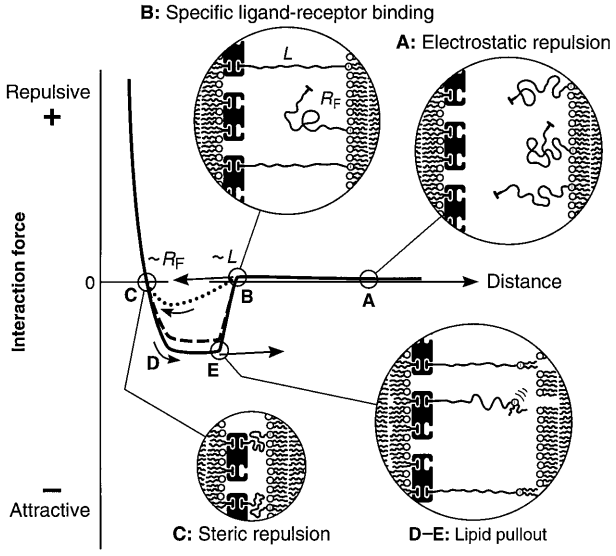

Fig. 3. Schematic construction of the "ideal" tethered ligand-receptor interaction potential. (**A**) At large separation distances, the interaction is a double-layer electrostatic repulsion. (**B**) Biotin molecules attached to PEG at near-full extension are able to "lock" into the biotin binding site. The minimum of the attractive potential on approach is determined by the coil elastic restoring force, Eq. 7, and is close to R_F. (**C**) Coil steric repulsion acts over a range of $D < R_F$. (**D** and **E**) The effective separation potential (solid line) is determined by the strength of lipid pullout or ligand-receptor bond (whichever is weakest—here lipid pullout, dashed line) and the polymer coil interaction (dotted line), and acts over a range of the fully extended tether length, L.

generic to all tethered ligand-receptor interactions if, as is usually the case, the strength of the ligand-receptor bond exceeds the strength of the anchoring membrane or molecule (*10*, *12*). Consider two surfaces that are to be separated after being brought together to a separation D_0. Initially, all tethers within a certain radius r_0 (or a certain fraction of tethers) are locked onto the other surface (Fig. 1B), where r_0 is related to D_0, R, and L by the Chord theorem (*13*):

$$r_0^2 = 2R(L - D_0) \quad (4)$$

Because the outermost tethers at $r = r_0$ are fully stretched, these molecules will be pulled out from the membrane as soon as the surfaces begin to separate, and PEG-lipid pullout will continue until D reaches the value of $(D_0 + \ell)$, where ℓ is the lipid chain length. The total force, due to lipid pullout only, to separate the two surfaces from $D = D_0$ to $D = (D_0 + \ell)$ scales directly with the active area (Fig. 1B) and is given by

$$F(D) = -2\pi R(D - D_0)\sigma f F_{lip}$$
$$\text{Regime 1: } D = D_0 \text{ to } (D_0 + \ell) \quad (5)$$

where σ is the surface coverage of PEG-biotin, and f is the fraction of PEG-biotin molecules attached to streptavidin. This is the first regime, corresponding to the path C → D in the dashed force curve of Fig. 3. Inserting the relevant values for these experiments [$R = 1.32$ cm, $\sigma = 10^{17}$ m^{-2}, $f = 0.1$ (*4*), $F_{lip} = 23$ pN (*11*)] into Eq. 5 gives a steep constant slope in F/R of $-2\pi\sigma f F_{lip} \approx 1.5 \times 10^6$ N m^{-1}, compared with the measured slope of 4×10^6 N m^{-1} (Fig. 2).

At $D > (D_0 + \ell)$ another regime takes over until $D = L$. In this regime the outermost lipids are continually being plucked out from the membrane (in contrast to the first regime where they are still partially inside the membrane), whereas the innermost lipid tethers are still not fully stretched. The force law for lipid pullout in this second regime is

$$F(D) = -2\pi R\ell\sigma f F_{lip}$$
$$\text{Regime 2: } D = (D_0 + \ell) \text{ to } L \quad (6)$$

This force is independent of D and thus constant. Inserting the appropriate values ($\ell = 28$ Å, and so forth) into Eq. 6 gives $F/R \approx 4.4$ mN m^{-1} for the lipid pullout contribution in this regime. This value may be compared with the measured value of 8 mN m^{-1} (Fig. 2 and Fig. 3, D → E), which includes contributions from the maximum polymer force between the surfaces given by

$$\frac{F_{ext}(D \approx R_F)}{R} \approx -\pi f\sigma kT\left(\frac{L}{R_F^2}\right)$$
$$\approx -2.8 \text{ mN m}^{-1} \quad (7)$$

In the third and last regime, starting at $D = L$, all of the PEG lipids are fully stretched and the outermost ones are continually being plucked out from the membrane until the last one leaves when $D = (L + \ell)$. The force law in the third regime is

$$F(D) = -2\pi R(L + \ell - D)\sigma f F_{lip}$$
$$\text{Regime 3: } D = L \text{ to } (L + \ell) \quad (8)$$

which gives a force with a constant slope of $+2\pi R\sigma f F_{lip} \approx 2 \times 10^4$ N m^{-1} and is equal to that in regime 1 but of opposite sign. Because this slope is now positive, at the turning point (Fig. 3, point E), the surfaces "jump out" of their potential well (*7*).

The above analysis appears to explain, both qualitatively and quantitatively, the measured interaction potential. Although the exact numbers are system-dependent, a similar type of interaction potential (depicted schematically in Fig. 3) can be expected to apply to many different types of complementary interactions. The "tethered potential" exhibits a number of interesting features, especially when compared with the "basic" short-range (<5 Å) interaction of the untethered biotin-streptavidin ligand-receptor pair (Fig. 2, solid curve) (*14*). First, the tether markedly extended the range of the interaction (experimentally, we found ≈150 Å) (*15*). Second, although the adhesive force (regime 2) in the high-affinity streptavidin-biotin system was determined by lipid pullout, the total energy of the interaction was set by the distance over which the force acted. Hence, in other lower affinity cases with a tether, the total energy will be controlled by both the ligand-receptor bond energy and the length of the tether.

In terms of general biological interactions, this may be another means of regulating the time and length scales of the binding process independently of the specific ligand-receptor affinity (an important point because tethered ligands are currently being exploited for use in drug delivery systems and tissue engineering applications). Our results demonstrate that the addition of a flexible molecular tether extends the effective range of a specific ligand-receptor interaction by the length of the fully extended chain, and thus that the effective receptor-ligand on-rate is controlled by the tether length and dynamics.

REFERENCES AND NOTES

1. G. Blume *et al*., *Biochim. Biophys. Acta* **1149**, 180 (1993); T. M. Allen, E. Brandeis, C. B. Hansen, G. Y. Kao, S. Zalipsky, *ibid.* **1237**, 99 (1995); S. A. DeFrees, L. Phillips, L. Guo, S. Zalipsky, *J. Am. Chem. Soc.* **118**, 6101 (1996); S. Zalipsky, B. Puntambekar, P. Boulikas, C. M. Engbers, M. C. Woodle, *Bioconjugate Chem.* **6**, 705 (1995); R. J. Lee and P. S. Low, *J. Biol. Chem.* **269**, 3198 (1994).
2. D. Papahadjopoulos *et al*., *Proc. Natl. Acad. Sci. U.S.A.* **88**, 11460 (1991).
3. T. L. Kuhl, D. E. Leckband, D. D. Lasic, J. N. Israelachvili, *Biophys. J.* **66**, 1479 (1994).
4. D. E. Leckband, F.-J. Schmitt, J. N. Israelachvili, W. Knoll, *Biochemistry* **33**, 4611 (1994).
5. A solution of amino-PEG-DSPE {prepared from PEG-2000 [S. Zalipsky *et al*., *FEBS Lett.* **353**, 71 (1994)]} (300 mg, 0.11 mmol) and triethylamine (46 μl, 0.33 mmol) in chloroform (1.7 ml) was treated with the succinimidyl ester of biotin (41.31 mg, 0.121 mmol) predissolved in dimethyl formamide (300 μl). After 20 min of thin-layer chromatography (Silica Gel G, $CHCl_3/CH_3OH/H_2O$, 90:18:2) showed that the reaction was complete [R_f values of 0.47 and 0.51 for distearoylphosphatidylethanolamine (DSPE)-PEG-NH_2 and biotin-PEG-DSPE, respectively], the reaction mixture was filtered and loaded onto the silica gel column. The product was eluted with a stepwise gradient of methanol (0 to 14% v/v) in chloroform (2% increments every 50 ml). The product-containing fractions were pulled and evaporated to dryness. The residue was dissolved in *tert*-butanol and lyophilized, yielding a white powder, 196 mg (60%). ^{1}H-nuclear magnetic resonance (CD_3OD): δ 0.88 (t, CH_3, 6H), 1.26 (s, CH_2, 56H), 1.45 (m, CH_2 biot., 2H), 1.58 (br m, $CH_2CH_2C{=}O$ 4H of each lipid and biot.), 3.20 (m, SCH biotin and CH_2NH of PEG, 3H), 3.53 (t, CH_2NH of PE, 2H), 3.64 (s, PEG, ≈ 180H), 3.88 and 3.98 (q and t, $CH_2PO_4CH_2$, 4H), 4.20 (t, CH_2O_2CN, 2H), 4.17 and 4.39 (2x dd, OCH_2CHCH_2OP, 2H), 4.3 and 4.5 (2x dd, CHNH-CONHCH, 2H), 5.2 (m, $PO_4CH_2CHCH_2OP$, 1H).
6. J. Marra and J. Israelachvili, *Methods Enzymol.* **127**, 353 (1986).
7. The surfaces jump in or out whenever the gradient of the force exceeds the mechanical restoring force (here, the spring constant of the apparatus).
8. The true potential is actually closer to a Langevin function and at 10% below full extension is likely to be larger than the parabolic potential. Although the freely hinged potential is more accurate, the quadratic form (Kramer's type approximation) is a good approximation for the following reasons: (i) the chains are barely overlapping, hence "brush effects" should be small; and (ii) the strongly stretched configurations make the chain interact even less with its neighbors.
9. For a chain in good solvent conditions, the polymer layer thickness $\langle x \rangle = \sqrt{\pi/2}N^{0.6}a \approx 43$ Å for PEG-2000, where N is the number of monomer units and a is the length of a monomer unit.
10. G. I. Bell, *Science* **200**, 618 (1978).
11. The force required to break a biotin-streptavidin bond is >130 pN [N. Green, *Methods Enzymol.* **184**, 51 (1990); V. T. Moy, E.-L. Florin, H. E. Gaub, *Science* **266**, 257 (1994)]. The force needed to pull out a PEG-lipid from a bilayer into water is ~16kT or 23 pN {[G. Cevc and D. Marsh, *Phospholipid Bilayers* (Wiley, New York, 1987)]; critical micellar concentration of MPEG1900-DSPE ≈ 5.8 μM [P. S. Uster *et al*., *FEBS Lett.* **386**, 243 (1996)]}.
12. E. Evans and K. Ritchie, *Biophys. J.*, in press.
13. J. Israelachvili, *Intermolecular and Surface Forces* (Academic Press, London, ed. 2, 1992).
14. Over biological time scales, the interaction was intrinsically irreversible and therefore a nonequilibrium one, where the interaction energy or force on approach was quite different from that on separation (compare with Fig. 3). Nonequilibrium effects are usually not discussed when considering complementary interactions. However, it is the energy or force on approach that determines the "on-rates" of binding reactions, whereas that on separation determines the "off-rate."
15. The particular dynamics or characteristic time of the tether coupled with the ligand receptor pair will ultimately determine the effective on- and off-rates.
16. See G. Cevc and D. Marsh, in (*11*).
17. D. E. Leckband, J. N. Israelachvili, F.-J. Schmitt, W. Knoll, *Science* **255**, 1419 (1992).

18. We thank P. Pincus, G. Fredrickson, and C. Marques for valuable discussions and D. McLaren for preparing the figures. J.Y.W. was supported by an NIH/National Research Service Award individual postdoctoral fellowship (GM17876). T.L.K. and J.N.I. were supported by NIH grant GM 47334.

6 September 1996; accepted 13 December 1996